4825

Ceiling Radiant Cooling Panels Employing Heat-Conducting Rails: Deriving the Governing Heat Transfer Equations

Yizai Xia, PhD
Member ASHRAE

Stanley A. Mumma, PhD, PE
Fellow ASHRAE

ABSTRACT

The central thrust of this paper is the derivation of the governing heat transfer equations for a ceiling radiant cooling panel (CRCP) that employs an extruded aluminum heat-conducting rail (HCR) between the copper tube waterway and the ceiling to room heat transfer metal sheet. The utility of the derived governing heat transfer equations to predict the performance of CRCPs using HCRs with various geometries, materials of construction, fluid inlet temperatures and flow rates, and room environments—including mechanically induced forced convection—is also presented.

INTRODUCTION

There are three principal types of overhead hydronic radiant cooling systems: concrete core ceilings, lightweight metal ceiling radiant cooling panels (CRCP), and capillary tube cooling grids embedded in plaster ceilings. This paper focuses on the metal CRCP design. Many metal CRCPs employ extruded aluminum sections as heat transfer receivers, with copper tubes thermally and mechanically connected to the extrusion then top loaded with an insulating blanket. An alternate CRCP design employs a thin, cold-rolled metal sheet as the heat transfer receiver. In order to enhance the alternate CRCP's heat transfer performance, an extruded aluminum heat-conducting rail (HCR), as shown in Figure 1, is used. The thermal resistance between the tubes and the HCR is reduced through the use of a heat sink paste. The HCR must also be well bonded to the metal sheet to minimize thermal resistance; however, since the contact area is large, this bonding is less important than that of the tube to HCR thermal connection. The alternate design also is top loaded with an insulating blanket. In summary, the CRCP design to be analyzed in this paper consists of the metal sheet heat receiver, HCRs, copper tube waterways, and top insulation.

Many factors influence the capacity of CRCPs, including component materials and configurations, operating flow and temperatures, and space thermal temperatures and air flow patterns. This work was undertaken because a full literature review has revealed that nothing currently exists to analytically address the performance of CRCPs employing HCRs.

The equations for CRCPs without HCRs have been described by Conroy and Mumma (2001). In this paper, their equations are extended so that a CRCP with HCRs can be thermally analyzed.

DERIVATION OF THE GOVERNING HEAT TRANSFER EQUATIONS

Consider the CRCP configuration shown in Figure 1. The governing heat transfer equations are derived using the following assumptions:

1. Heat is absorbed on the downward-facing surface of the CRCP metal sheet, and the top surface of the metal sheet-HCR-copper tube waterway assembly is insulated and treated as adiabatic.
2. All hydronic circuits are identical and parallel.
3. The flow is fully developed.
4. For fin sections 1 and 2 (see Figure 1), the temperature gradients are assumed to be one-dimensional because the Biot number (ratio of heat transfer by convection to the downward-facing metal sheet to the heat transfer by conduction vertically in the fin sections) is far less than 1 due to the high thermal conductivity of the thin metal sheet.

Yizai Xia is research assistant and **Stanley A. Mumma** is a professor in the Department of Architectural Engineering at Penn State University, University Park, Pa.

5. The temperature at T_b is the local fin section 2 base temperature (see Figure 1) and is assumed to be equal to the outside tube wall temperature. This assumption is based upon the tube cradling design of the extruded aluminum HCR and the use of a high performance heat sink compound between the tube and the HCR.
6. The HCR is thermally bonded to the panel sheet sufficiently well so that at any position x the HCR and panel sheet temperatures are assumed equal.

The region between x equals zero (centerline between tubes) and $x = x_2$ (the tube base) can be considered a classical fin problem. It can be divided into two sections, from the centerline to x_1 (fin section 1) and from x_1 to x_2 (fin section 2, see Figure 1). By performing an energy balance on the two fin sections, the following ordinary differential equations, boundary conditions, and solutions are obtained.

Fin Section 1: $0 < x < x_1$
Governing equation

$$\frac{d^2T_1}{dx^2} - m_1^2 T_1 = -m_1^2 T_a\,, \qquad m_1 = \sqrt{\frac{U}{(k_1\delta_1)}} \tag{1}$$

Boundary conditions

$$\left.\frac{dT_1}{dx}\right|_{x=0} = 0, \qquad T_1\big|_{x=x_1} = T_j \tag{2}$$

Solution

$$T_1 = T_a + (T_j - T_a)\frac{\cosh(m_1 x)}{\cosh(m_1 x_1)} \tag{3}$$

Fin Section 2: $x_1 < x < x_2$
Governing equation

$$\frac{d^2T_2}{dx^2} - m_2^2 T_2 = -m_2^2 T_a\,, \qquad m_2 = \sqrt{\frac{U}{(k_1\delta_1 + k_2\delta_2)}} \tag{4}$$

Boundary conditions

$$T_2\big|_{x=x_1} = T_j\,, \qquad T_2\big|_{x=x_2} = T_b \tag{5}$$

Solution

$$T_2 = T_a + d\sinh(m_2 x) + e\cosh(m_2 x) \tag{6}$$

where

$$d = [(T_b - T_a)\cosh(m_2 x_1) + (T_a - T_j)\cosh(m_2 x_2)]/\sinh(m_2 W_{HCR})$$
$$e = [(T_a - T_b)\sinh(m_2 x_1) + (T_j - T_a)\sinh(m_2 x_2)]/\sinh(m_2 W_{HCR})$$

The temperature at the edge of the HCR, T_j, can be obtained from the assumption that the heat flux at $x = x_1$ is the same in each section. This is represented by Equation 7. It assumes that the heat transfer at x_1^+ is one dimensional and is considered reasonable because the HCR is thin.

$$k_1\delta_1 \left.\frac{dT_1}{dx}\right|_{x=x_1} = (k_1\delta_1 + k_2\delta_2)\left.\frac{dT_2}{dx}\right|_{x=x_1} \tag{7}$$

Then

$$T_j = T_a - \frac{T_a - T_b}{g} \tag{8}$$

where

$$g = \cosh(m_2 \cdot W_{HCR}) + \sinh(m_2 \cdot W_{HCR}) \cdot \tanh(m_1 \cdot x_1) \cdot (k_1\delta_1 m_1)/(k_1\delta_1 + k_2\delta_2)m_2$$

The total heat gained by the CRCP for one tube per unit of length q' in the flow direction includes two parts. They are the energy collected below the tube region, as shown in Equation 10, and the useful gain by the region between two tubes, as shown in Equation 11.

$$q' = q'_{tube} + q'_{fin} \tag{9}$$

$$q'_{tube} = D_o U(T_a - T_b) \tag{10}$$

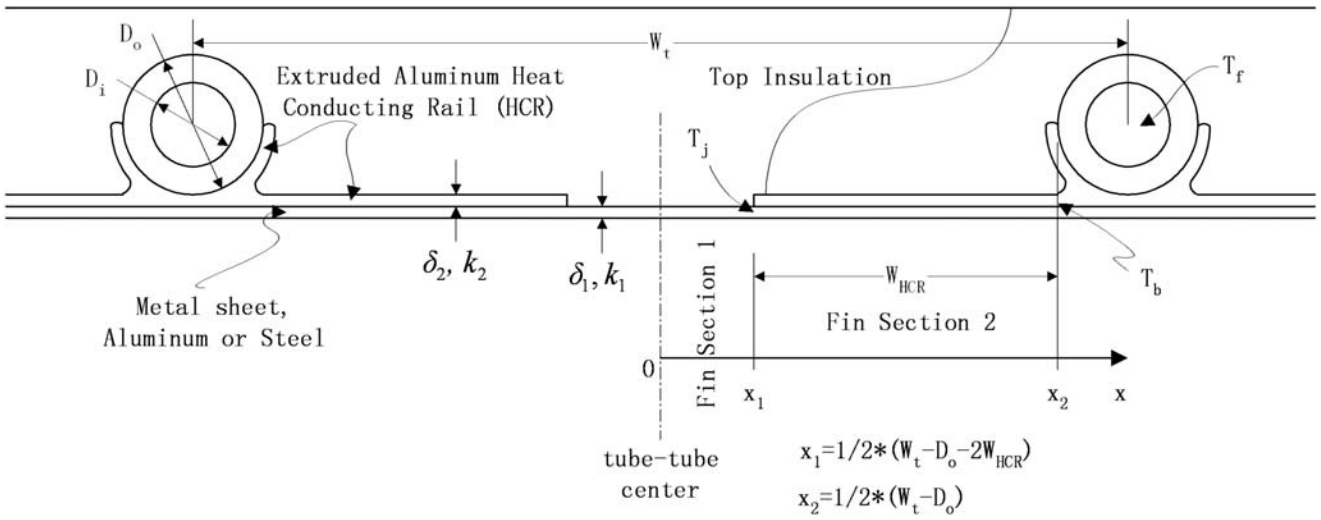

Figure 1 *Schematic of CRCP geometry and nomenclature.*

$$q'_{fin} = -2(k_1\delta_1 + k_2\delta_2)\left.\frac{dT_2}{dx}\right|_{x=x_2} = 2(k_1\delta_1 + k_2\delta_2)m_2\frac{T_j - T_a + (T_a - T_b)\cosh(m_2 W_{HCR})}{\sinh(m_2 W_{HCR})} \quad (11)$$

Ultimately, the heat transferred from the room to the CRCP is transferred to the fluid via the tube to fluid resistance and the tube to HCR bond conductance as expressed in Equation 12. Because of the HCR geometry and the use of the heat sink compound between the HCR and the tube, it is assumed in this paper that the tube to HCR bond conductance is greater than 30 W/m·°C (17 Btu/h·ft·°F).

$$q' = \frac{T_b - T_f}{\frac{1}{h_{fi}\pi D_i} + \frac{1}{C_b}} \quad (12)$$

Note: The unique and most important equations derived in this paper are Equations (1-12).

The heat transfer coefficient between the fluid and the tube wall h_{fi} is evaluated using Equation 13 (Lienhard IV and Lienhard V 2003). The flow is assumed laminar for Reynolds numbers below 2300.

$$h_{fi} = \mathrm{Nu} \cdot k / D_i \quad (13)$$

when Re < 2300

$$\mathrm{Nu} = 3.657$$

when Re > 2300

$$\mathrm{Nu} = \frac{(f/8)(\mathrm{Re} - 1000)\,\mathrm{Pr}}{1 + 12.7\sqrt{f/8}\left(\mathrm{Pr}^{\frac{2}{3}} - 1\right)}$$

$$f = \frac{1}{(1.82\log_{10}\mathrm{Re} - 1.64)^2}$$

Applying an energy balance to the fluid in the direction of flow yields the following equations (Duffie and Beckman 1991):

$$F' = \frac{q'}{-W_t U(T_f - T_a)} \quad (14)$$

$$T_{fo} = T_a + (T_{fi} - T_a)\exp[-A_c U F' / (\dot{m}_s C_p)] \quad (15)$$

$$Q_{cap} = \frac{\dot{m}_s C_p (T_{fo} - T_{fi})}{A_c} \quad (16)$$

$$F_R = \frac{Q_{cap}}{-U(T_{fi} - T_a)} \quad (17)$$

$$T_{fm} = T_{fi} + \frac{Q_{cap}}{F_R U}\left(1 - \frac{F_R}{F'}\right) \quad (18)$$

$$T_{pm} = T_{fi} + \frac{Q_{cap}}{F_R U}(1 - F_R) \quad (19)$$

F' is defined as the CRCP efficiency factor and represents the ratio of the actual energy gain to the useful gain that would occur if the metal sheet surface had been at the local fluid temperature. Finally, the CRCP heat removal factor, F_R, is an important indicator of the CPCR thermal performance. F_R is defined as the ratio of actual heat transfer to the heat transfer that would occur if the whole metal sheet surface were at the inlet fluid temperature, which is the maximum possible heat transfer. The mean fluid temperature T_{fm} is the proper temperature for evaluating fluid properties, while calculating the heat transfer coefficient $h_{fi} \cdot T_{pm}$ is the mean metal sheet surface temperature, which can be used to calculate the useful energy gain per unit area of the CRCP, or the CRCP capacity Q_{cap} (W/m^2) given by Equation 20.

$$Q_{cap} = U(T_a - T_{pm}) \quad (20)$$

The CRCP total energy gain has two components—radiant heat flux and convective heat flux, as characterized by Equation 21.

$$Q_{cap} = h_c(T_a - T_{pm}) + h_r(AUST - T_{pm}) \quad (21)$$

By substituting Equation 21 into Equation 20, the overall heat transfer coefficient between the CRCP and the conditioned space is obtained, Equation 22:

$$U = h_c + h_r\frac{AUST - T_{pm}}{T_a - T_{pm}} \quad (22)$$

To simplify the analysis, a linearized radiant heat transfer coefficient is defined by Equation 23.

$$h_r = 5\times10^{-8}[(AUST + 273)^2 + (T_{pm} + 273)^2] \cdot [(AUST + 273) + (T_{pm} + 273)] \quad (23)$$

The area-averaged uncontrolled room surface temperature (AUST) can be evaluated using Equation 24, as suggested by Kilkis (1995).

$$AUST = T_a - Index \cdot (7/(T_o - 45)) \qquad \begin{matrix} 26°\mathrm{C} \le T_o \le 36°\mathrm{C} \\ 79°\mathrm{F} \le T_o \le 97°\mathrm{F} \end{matrix} \quad (24)$$

where *Index* is the room position index. *Index* is 0.5 for a room without outdoor exposure, 1.0 for a room with one outdoor exposed side and the fenestration area less than 5% of the total room surface area or 2.0 when the fenestration is more than 5%, and 3.0 for a room with two or more outdoor exposed sides.

Combined forced and natural convective heat transfer, or mixed convective heat transfer, at the CRCP surface has been discussed by Awbi and Hatton (2000) and Jeong and Mumma (2003). Using the correlation suggested by Awbi and Hatton (2000), the semi-empirical Equation 25 is presented for a diffuser located on a wall near the ceiling whose discharged air velocity varies between 0.4 and 2.1 m/s (78.7 and 413.4 fpm).

$$h_c = (h_{cn}^{3.2} + h_{cf}^{3.2})^{\frac{1}{3.2}}$$
$$h_{cn} = \frac{2.175}{D_e^{0.076}}(T_a - T_{pm})^{0.308} \quad (25)$$
$$h_{cf} = 4.248 \cdot W_{diff}^{0.575} \cdot V^{0.557}$$

The entire set of equations presented above can be solved iteratively with a reasonable trial value of T_{pm}.

PARAMETRIC ANALYSIS

The utility of the CRCP governing heat transfer equations derived in this paper will now be illustrated. The many variables that influence the CRCP cooling capacity can be classified into two major categories:

- ***CRCP characteristics*:** tube center-to-center spacing (W_t), width and thickness of the heat-conducting rail (W_{HCR}, δ_2), tube diameter (D_i, D_o), CRCP length (L), metal sheet and tubing thermal physical properties, metal sheet thickness (δ_1) and thermal conductivity (k_1), mass flow rate of water per tube ($\dot{m}_s$), and inlet water temperature (T_{fi}).

- ***Application characteristics*:** room design dry-bulb temperature (T_a), room dew-point temperature (sets lower limit for T_{fi}), summer outdoor dry-bulb temperature (T_o), room position index (*Index*), and diffuser discharged air velocity (V).

In order to facilitate a comparative analysis, a base case representative of commercial products is defined and presented in Table 1. For the conditions of Table 1, the mean metal sheet surface temperature is 17°C (63°F) and the CRCP capacity is about 83 W/m^2 (26 Btu/h·ft^2).

In the analysis that follows, CRCP variable excursions away from the base case are generally limited to the several being explored at the time. All variables are returned to their base case values before exploring the influence of other variables.

HCR Ratio and Tube Diameter

The temperature distribution along the fin perpendicular to the copper tube for various HCR ratios is presented in Figure 2 (note the abrupt change in the fin temperature distribution at T_j, i.e., between fin sections 1 and 2). The HCR ratio is defined as the fraction of the metal sheet surface area covered with the HCRs and is expressed as

$$\text{HCR ratio} = (W_{HCR} + D_o/2)/(W_t/2). \quad (26)$$

The overall metal sheet surface temperature decreases as the width of the HCR increases.

To further investigate the impact of the HCR ratio on the CRCP cooling capacity, two important capacity-related variables that appear in the Q_{cap} equations (Equations 17 and 20), F_R and T_{pm}, were chosen for study. Figure 3 illustrates how F_R, and hence Q_{cap}, increases with increasing HCR ratios to a virtual maximum for a HCR ratio of 0.75 (i.e., 75% of the entire metal sheet surface area is covered with HCRs). T_{pm} decreases with increasing HCR ratio as well (also indicating an increase in Q_{cap}), then levels out. Further increases in the width of the HCR would simply increase the cost without improving Q_{cap}.

The effect of HCR thickness on the CRCP capacity is also investigated. Increasing the thickness of the HCR decreases the metal sheet surface temperature, causing the Q_{cap} to increase. The increases in the heat removal factor and the cooling capacity are as expected.

Standard CRCP tube diameters from 8 to 20 mm (0.3 to 0.8 in.) were also selected for study. It was found that the heat removal factor increases with increasing tube diameter for constant tube spacing.

Tube Center-to-Center Spacing and Mass Flow Rate of Water

Figure 4 illustrates the effects of tube center-to-center spacing, W_t, and mass flow rate of water. As the mass flow rate of water through a tube increases from 0.01 Kg/s (1.32 lb/min) into 0.05 Kg/s (6.61 lb/min), the flow transitions from laminar to turbulent. Figure 4(a) is for a laminar flow case (Reynolds number of approximately 1020), while Figure 4(b) is for a turbulent flow case (Reynolds number of approximately 5100). As one might expect, increasing the HCR ratio increases the CRCP performance (F_R) more significantly for turbulent flow than laminar flow.

Table 1. Base Case CRCP Design

W_t, m (ft)	W_{HCR}, m (ft)	HCR ratio	δ_1, mm (in.)	δ_2, mm (in.)	D_i, mm (in.)	D_o, mm (in.)	L, m (ft)	$\dot{m}_s$, kg/s (lb/min)
0.2 (7.9)	0.05 (1.97)	0.625	1 (0.04)	1 (0.04)	10.5 (0.4)	12.5 (0.5)	4 (13)	0.01 (1.32)
T_a, °C (°F)	T_o, °C (°F)	V, m/s (ft/min)	T_{fi}, °C (°F)	*Index*	CRCP Material			
26 (79)	30 (86)	0 (0)	13 (55)	1	Aluminum metal sheet, HCR, and copper tube			

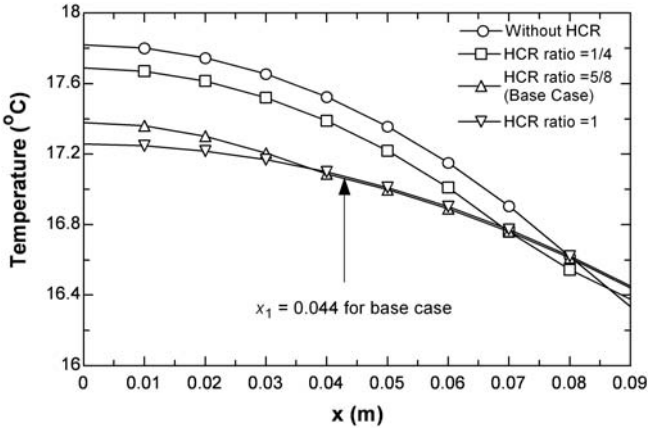

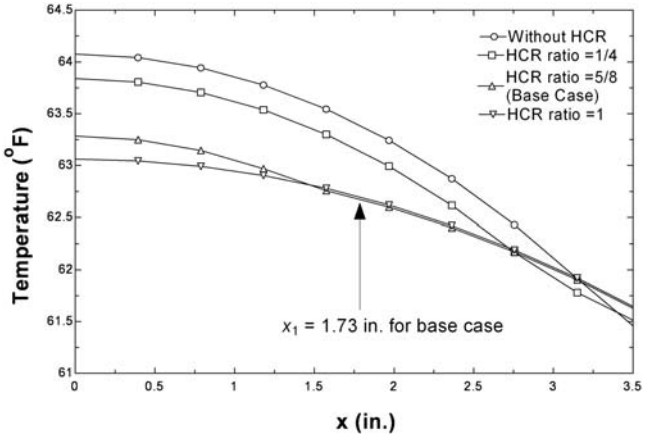

Figure 2 *Fin temperature distribution for different HCR ratios.*

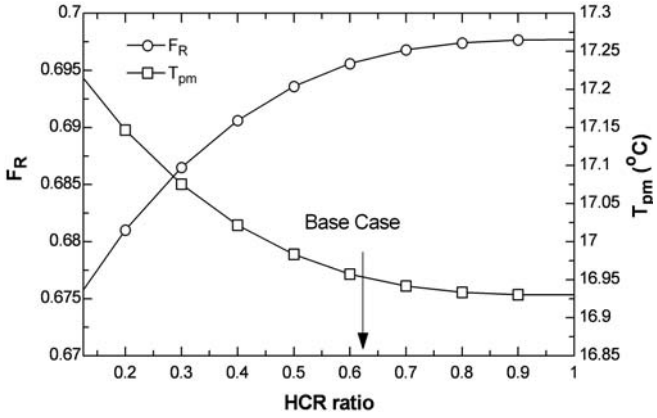

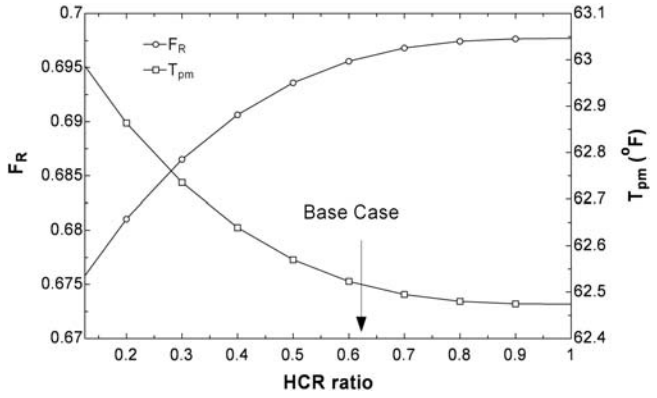

Figure 3 *HCR ratio vs. CRCP heat removal factor F_R and mean metal sheet surface temperature T_{pm}.*

For both laminar and turbulent flow, as the tube center-to-center spacing increases, HCRs become more and more beneficial. HCRs can significantly increase the heat removal factor F_R and the capacity of the CRCP. For instance, when the tube spacing is 0.5 m (1.6 ft), a HCR ratio of 0.75 will increase the heat removal factor and CRCP capacity by about 10% and 15% for laminar and turbulent flow, respectively.

Tube Length

Since the fluid temperature increases in the flow direction, the mean metal sheet surface temperature increases as the tube length increases for a given mass flow rate per tube. Consequently, there is a decrease in the cooling capacity of the CRCP. On average, for laminar flow, Q_{cap} decreases by 16% as the tube length is increased from 3 to 10 m (10 to 33 ft). For turbulent flow, the average decrease in Q_{cap} as the tube length is increased from 3 to 10 m (10 to 33 ft) is 3.5%. Laminar flow should be avoided.

Metal Sheet Material

In practice, the metal sheet may be either steel or aluminum. Because the thermal conductivity of aluminum is almost six times that of steel, CRCPs employing steel metal sheets have lower cooling capacity than those employing aluminum metal sheets of equal geometry and thickness. Figure 5 presents the heat removal factors of the aluminum and steel metal sheets plus HCR for different tube spacing. The reduction in F_R when a steel metal sheet is used is about 4% for W_t = 0.1 m (3.9 in.) and 28% for W_t = 0.5 m (19.7 in.).

Convective Heat Transfer Coefficient Inside the Tube

The thermal resistance between the tube wall and the fluid plays an important role in the performance of the CRCP and can be expressed as

$$r_{tube} = 1/(h_f \pi D_i)\,. \tag{27}$$

To investigate the impact of h_{fi} on CRCP cooling capacity, a series of values of h_{fi} from 100 to 3000 W/m^2·°C (17.6 to 528.4 Btu/h·ft^2·°F) were chosen and presented in Figure 6. As

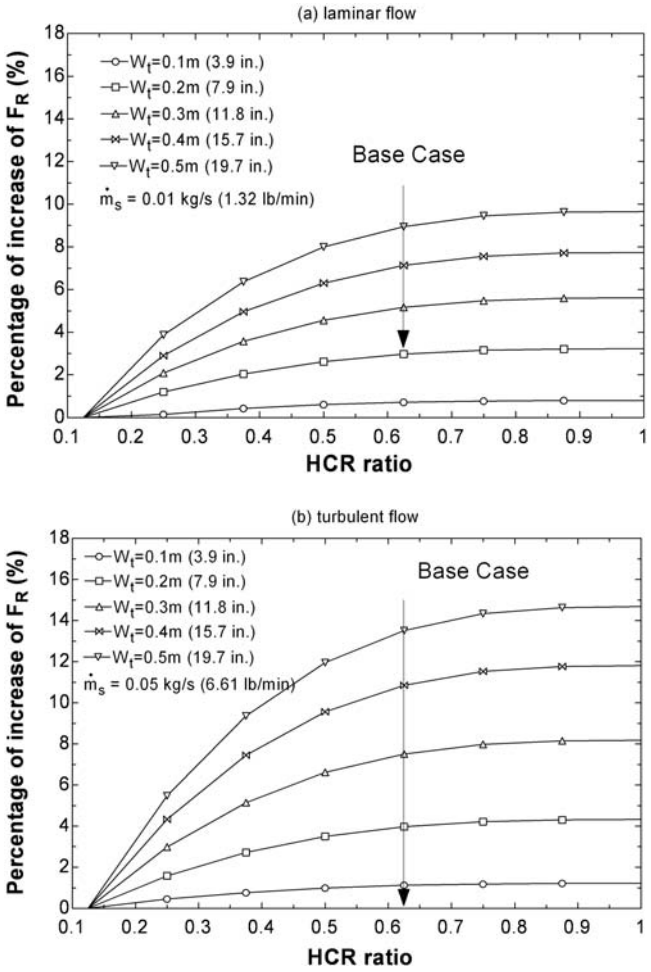

Figure 4 *Percent F_R increase vs. HCR ratio for different tube center-to-center spacing and mass flow (laminar and turbulent cases).*

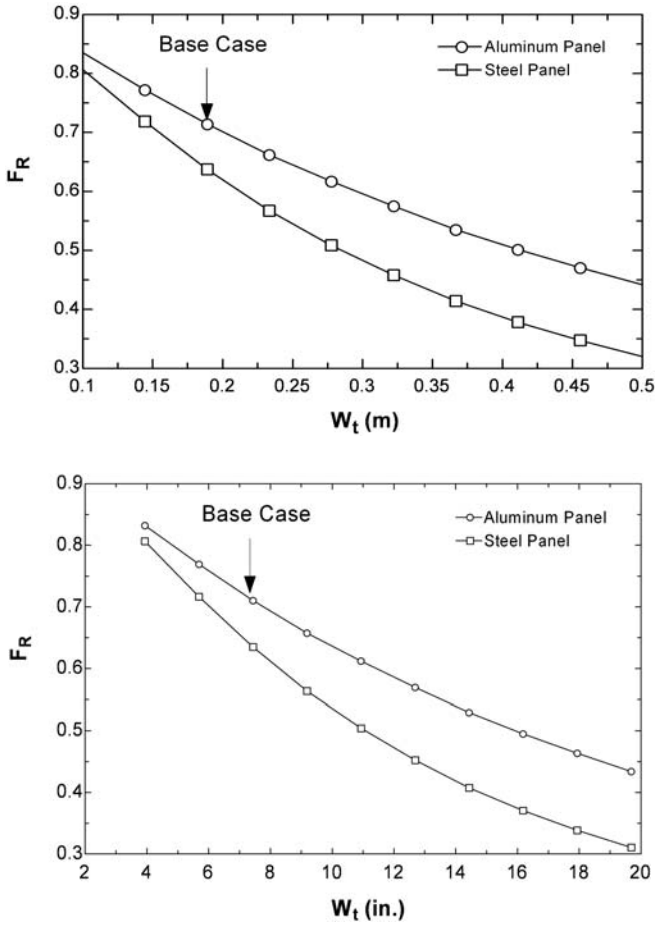

Figure 5 *Heat removal factors for aluminum and steel metal sheet vs. tube to tube spacing.*

expected, the CRCP capacity increases and the mean metal sheet surface temperature decreases with increasing heat transfer coefficients. Note that increasing h_{fi} beyond 2500 W/m^2·°C (440 Btu/h·ft^2·°F) does not result in significant increases in the CRCP cooling capacity.

Air-Side Mixed Convection on the CRCP

Air-side mixed convective heat transfer (natural and forced) can increase the CRCP capacity. The mixed convection coefficient proposed by Awbi (1998) was used in this paper's governing heat transfer equations to investigate the effects of overhead diffuser discharge air velocity on the CRCP total and radiant cooling capacity. The results are presented in Figure 7. With the addition of forced convection, the CRCP capacity increases, while the radiant part of the CRCP capacity is unaffected. In addition, the CRCP capacity increases nearly linearly with the temperature difference between the room air and the CRCP.

Figure 8 illustrates the relationship between forced convection (at various diffuser discharge velocities) and the room to metal sheet surface temperature differentials on the overall heat transfer. As expected, with increasing velocity, the CRCP heat transfer increases due to forced convection. However, as the room to metal sheet surface temperature differential increases, so does the natural convection. Consequently, the impact of forced convection is a little less significant at greater room to metal sheet surface temperature differences. When the diffuser discharge velocity is 1 m/s (197 fpm), the cooling capacity increases about 4% over natural convection. The heat transfer is enhanced approximately 11~15% over natural convection when the diffuser discharge velocity is 2 m/s (394 fpm). The result agrees with published experimental room tests, which indicate air-side mixed convection can increase the CRCP capacity by 10~15% (Kochendorfer 1996). The mixed convective coefficient obtained experimentally by Awbi and Hatton (2000) was for velocities less than 2.1 m/s (413.4 fpm). At the risk of extrapolating beyond his correlations, the effect of diffuser discharge

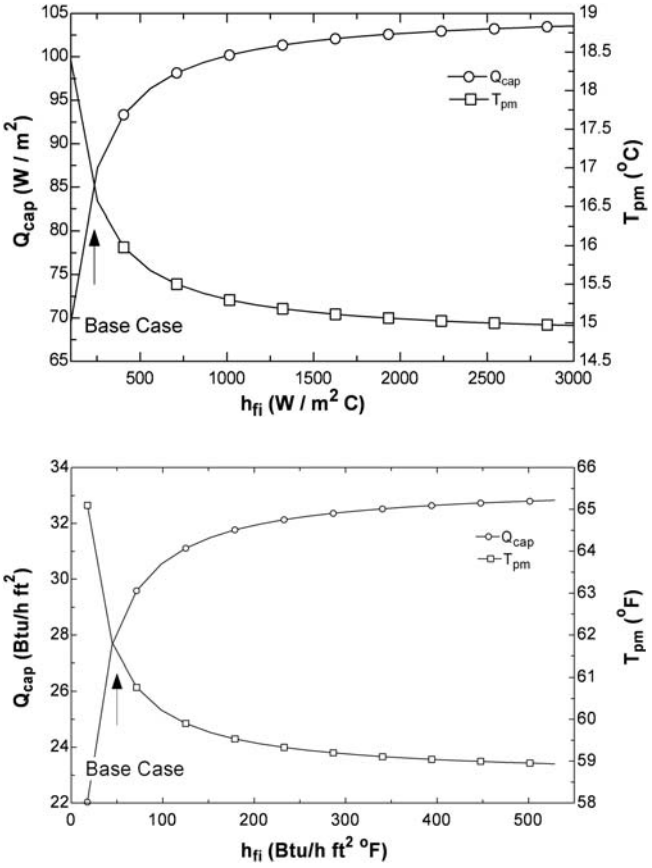

Figure 6 *Effect of tube inside convective heat transfer coefficient on CRCP capacity and mean metal sheet surface temperature.*

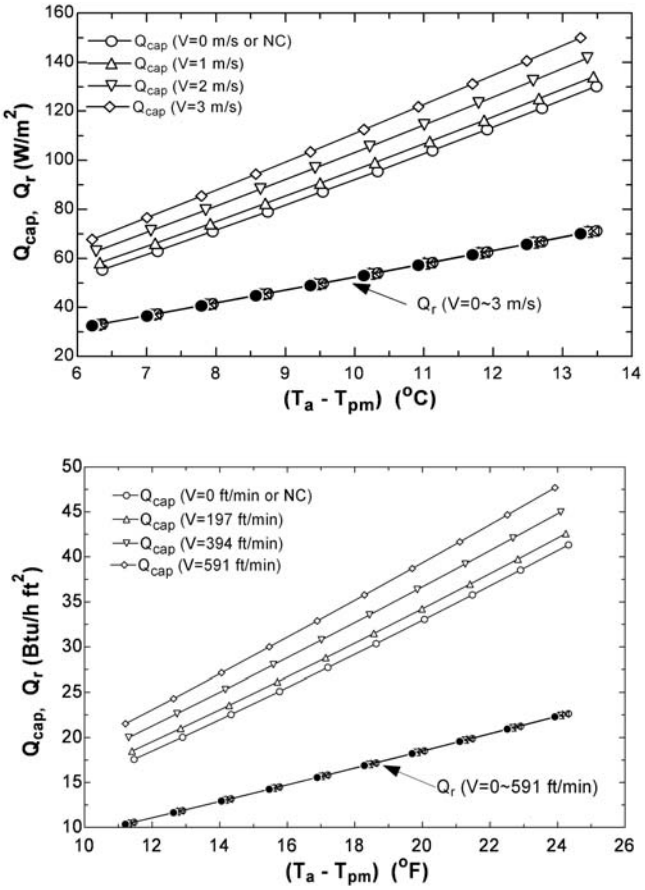

Figure 7 *CRCP total and radiant cooling capacity vs. room to metal sheets surface temperature differentials for air side mixed convection conditions. (turbulent liquid flow in tubes).*

velocities of 3 m/s (591 fpm) on the cooling capacity is evaluated using his correlation. The percentage increase in CRCP capacity with a diffuser discharge velocity of 3 m/s is about 18~24% for room to panel temperature differences of 7~13°C (12~23°F).

CONCLUSIONS

The following conclusions can be drawn from a parametric analysis using the governing heat transfer equations derived in this paper:

1. The addition of HCRs can effectively reduce the temperature of the metal sheet surface, thus increasing the CRCP capacity, especially when the tube-to-tube spacing is large and the tube fluid flow is turbulent.
2. When the HCR ratio reaches 0.75, its benefit reaches an asymptotic plateau for the CRCP configuration analyzed in this paper. Further increasing the HCR ratio does not result in significant benefit.
3. A CRCP employing an aluminum metal sheet has greater cooling capacity than one employing a steel metal sheet of comparable geometry. The performance differences increase as the tube-to-tube spacing increases.
4. Increasing the heat transfer coefficient between the fluid and the tube wall, h_{fi} , beyond 2500 W/m^2·°C (440 Btu/h·ft^2·°F) does not result in significant increases in the panel cooling capacity.
5. With the introduction of mechanically induced forced convection, the CRCP capacity increases 11~15%, compared to still air, for a diffuser discharge velocity of 2 m/s (394 fpm) when the room to metal sheet surface temperature differentials range 7~13°C (12~23°F). The CRCP capacity appears to be increased by 18~24% at diffuser discharge velocities of 3 m/s (591 fpm) compared to still air.

NOMENCLATURE

A_c = collector area, m^2

AUST = area-averaged temperature of uncontrolled surfaces, °C

C_b = bond conductance, W/m · K

D = diameter, m

D_e = hydraulic diameter of room surface, m

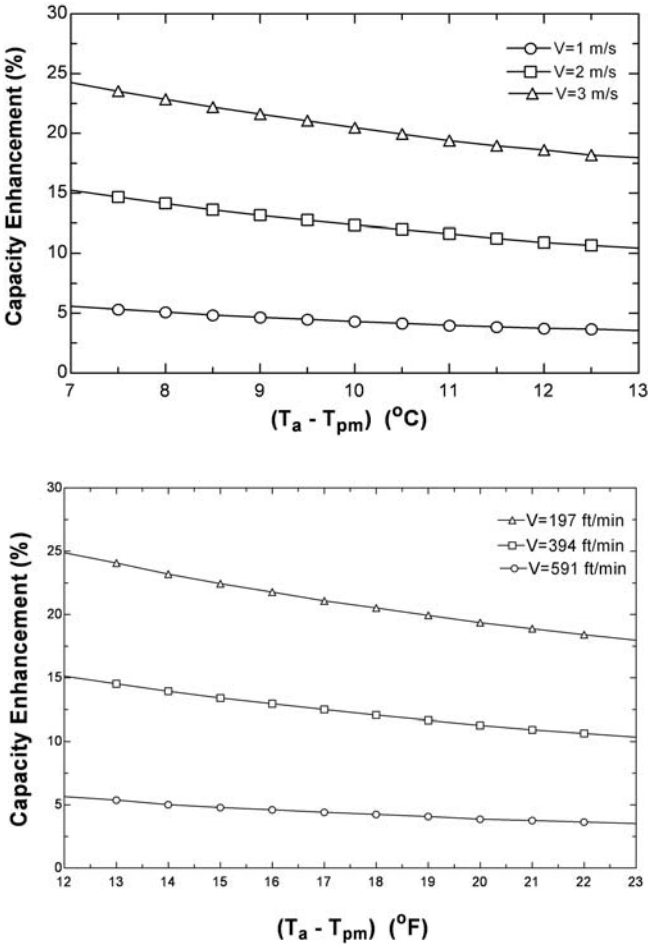

Figure 8 *CRCP capacity enhancement with air side mixed convection vs. room to metal sheet surface temperature differentials.*

f = friction factor
F' = CRCP efficiency factor
F_R = CRCP heat removal factor
h = heat transfer coefficient, W/m^2 · K
Index = room position index
k = thermal conductivity, W/m · K
$\dot{m}_s$ = mass flow rate of fluid per tube, kg/s
Nu = Nusselt number
Pr = Prandtl number
q' = heat gain per tube of the CRCP per unit of length, W/m
Q_{cap} = CRCP capacity, W/m^2
Re = Reynolds number
T = temperature, °C
U = overall heat transfer coefficient, W/m^2 · K
V = diffuser discharge air velocity, m/s
W = width, m
δ = metal sheet or HCR thickness, m

Subscripts

a = indoor air
b = bond or base
c = convection
cf = forced convection
cn = natural convection
diff = diffuser
f = fluid
i = inside or inlet
m = mean
o = outside or outlet
p = metal sheet
r = radiation
t = tube
1 = fin section 1
2 = fin section 2

REFERENCES

Awbi, H.B., and A. Hatton. 2000. Mixed convection from heated room surfaces. *Energy and Buildings* 32:153–166.

Conroy, C.L., and S.A. Mumma. 2001. Ceiling radiant cooling panels as a viable distributed parallel sensible cooling technology integrated with dedicated outdoor air systems. *ASHRAE Transactions* 107(1):578–585.

Duffie, J.A., and W.A. Beckman. 1991. *Solar Engineering of Thermal Processes*, 2d ed. New York: Wiley Interscience.

Jeong, J., and S.A. Mumma. 2003. Ceiling radiant cooling panel capacity enhanced by mixed convection in mechanically ventilated spaces. *Applied Thermal Engineering* 23:2293–2306.

Kilkis, B.I. 1995. COOLP: A computer program for the design and analysis of ceiling cooling panels. *ASHRAE Transactions* 101(2):703–710.

Kochendorfer, C. 1996. Standardized testing of cooling panels and their use in system planning. *ASHRAE Transactions* 102(1):651–658.

Lienhard, J.H. IV, and J.H. Lienhard V. 2003. *A Heat Transfer Textbook*, 3d ed. Cambridge: Phlogiston.